



# Magnetic hysteresis in the first order adiabatic phase transition of mesoscopic-size Type I superconductors

Peter D. Keefe<sup>a</sup>

College of Engineering and Science, University of Detroit Mercy, Detroit, MI 48221, USA

Received 18 August 2020 / Accepted 2 March 2021  
© The Author(s) 2021

**Abstract** Macroscopic and mesoscopic-size Type I superconductors exhibit a first order phase transition in  $H$ - $T$  space. For specimens undergoing an adiabatic phase transition, the latent heat is supplied or absorbed by the normal regime. This process, the magneto-caloric effect, proceeds isentropically and for macroscopic-size specimens, through an intermediate state of superconductive and normal phase domains. For mesoscopic-size specimens, the intermediate state is precluded in view the specimen dimension and the range of coherence are commensurate. John Bardeen proposed the appearance of magnetic hysteresis prior to phase nucleation for the phase transition to proceed isentropically. This paper shows Bardeen's magnetic hysteresis is a consequence of positive interphase boundary surface energy.

## 1 Introduction

This paper arises from private communications between the Author and John Bardeen of the Loomis Laboratory, circa 1986–1987, concerning the physics of the first order adiabatic phase transition of mesoscopic-size Type I superconductors. In a letter to the Author, [1] reproduced in [2], Bardeen argued on thermodynamic principles that the adiabatic phase transition of a mesoscopic specimen from the normal phase to the superconductive phase can proceed isentropically from a starting temperature,  $T_1$ , to a lower, ending temperature,  $T_2$ , only if magnetic hysteresis manifests prior to phase nucleation, leaving the theoretical details to the Author.

Specifically, Bardeen forwarded a magnetic hysteresis superheating field,  $H_a$ , defined by:

$$H_a^2/8\pi = F_n(T_2) - F_s(T_1), \quad (1)$$

where  $F_n$  is the free energy per unit volume of the normal phase at  $T_2$  and  $F_s$  is the free energy per unit volume of the superconductive phase in zero magnetic field at  $T_1$ , and where phase nucleation at  $T_1$  commences at a superheating field,  $H_a$ , greater than the critical field at  $T_1$ ,  $H_1$ , i.e.,  $H_a > H_1$ , under the condition that the adiabatic phase transition proceeds isentropically; that is,  $S_s(T_1) = S_n(T_2)$ .<sup>1</sup>

Superheating and supercooling of the phase transition of macroscopic-size Type I superconductors have been frequently observed, but these effects always

involve irreversibility, such as Joule heating, and irreproducibility, as for example due to imperfections and fluctuations [3, 4]. The classic Ginzburg–Landau (G–L) approach to superheating involves a potential barrier to the phase transition that arises out of the interplay between an ordering parameter decreasing the Gibbs potential and an applied magnetic field increasing the Gibbs potential, the concept being first forwarded by Pippard [5].

However, Bardeen's magnetic hysteresis in the mesoscopic-size adiabatic phase transition does not follow the G–L/Pippard model in that the magnetic hysteresis Bardeen suggested, hereafter “Bardeen Hysteresis”, must be absolutely reproducible by rigorously conforming to specific magnetic field values in order for the phase transition to proceed isentropically [2].

This presents a problem: What unique mechanism underlies Bardeen Hysteresis?

As this paper will show, the answer lies in the interplay between the applied magnetic field diamagnetic screening energy and the minimum energy necessary to create an interphase boundary due to the presence of positive interphase boundary surface energy.

It is important to note that classical G–L/Pippard magnetic hysteresis can and will occur independently of Bardeen hysteresis; the underlying processes are completely different and independent of one another.

Interestingly, when the physics of macroscopic-size Type I superconductors became “complete” in the mid-1960s, investigators shifted to the mesoscopic-size via robust studies of the properties of superconductive thin films. The unexpected discovery of high  $T_c$  superconductors thereupon took center stage and has remained so to the present. This paper addresses a curiously over-

<sup>a</sup> e-mail: [pdk@ix.netcom.com](mailto:pdk@ix.netcom.com) (corresponding author)  
<sup>1</sup> Bardeen's letter contains a typo: “ $H_a$  must be greater than  $H_2$ .” should read, “ $H_a$  must be greater than  $H_1$ .”

looked aspect of Type I superconductor physics, and as such, the references are period contemporary.

In the discussion below, the various figures depict topical aspects of the thermodynamics of tin, a typical Type I superconductor, for which  $H_0 = 309$  gauss, where  $H_0$  is the critical magnetic field at zero temperature, and  $T_c = 3.72^\circ\text{K}$ , where  $T_c$  is the critical temperature at zero magnetic field. The figures are mutually drawn to scale (with the exception of Fig. 8). The calorimetric data for tin are from [8] and the indicated values are calculated from the standard thermodynamic equations of superconductivity [9].

## 2 Phase transitions of a Type I superconductor

The phase transition of a Type I superconductor from the superconductive phase to the normal phase may proceed isothermally or adiabatically, involving two state variables, magnetic field ( $H$ ) and temperature ( $T$ ).

In that the superelectrons correlate over a range of coherence,  $\xi$ , typically  $10^{-4}$  cm, specimen dimensionality is categorized in this paper as either *macroscopic*, where the specimen dimension is much larger than  $\xi$ , or *mesoscopic*, where the specimen dimension is commensurate with  $\xi$ . The macroscopic and mesoscopic phase transitions are both first order [6]. Parenthetically, in a third category, *microscopic*, where the specimen dimension is much smaller than  $\xi$ , the phase transition is second order [7].

### 2.1 Isothermal phase transition

The isothermal phase transition of a Type I superconductor from the superconductive phase to the normal phase requires application of a critical magnetic field and, because the entropy of the superconductive phase is lower than that of the normal phase, a latent heat supplied by a heat reservoir.

The field-temperature ( $H$ - $T$ ) space diagram for an isothermal phase transition of tin is shown at Fig. 1.

The dashed phase transition curve delineates the normal phase above and the superconductive phase below. The phase transition curve is well-known to be closely approximated by:

$$H_c = H_0(1 - T_i^2/T_c^2), \quad (2)$$

where  $H_c$  is the instantaneous critical magnetic field,  $H_0$  is the critical field at absolute zero,  $T_i$  is the instantaneous temperature and  $T_c$  is the critical temperature in zero magnetic field.

At  $T_1$ , a magnetic field is applied by an external source, increasing from zero to  $H_1$ . The magnetic field increase is accompanied by performance of magnetodynamic work per unit volume,  $W_{H_1}$ , owing to diamagnetic screening energy:

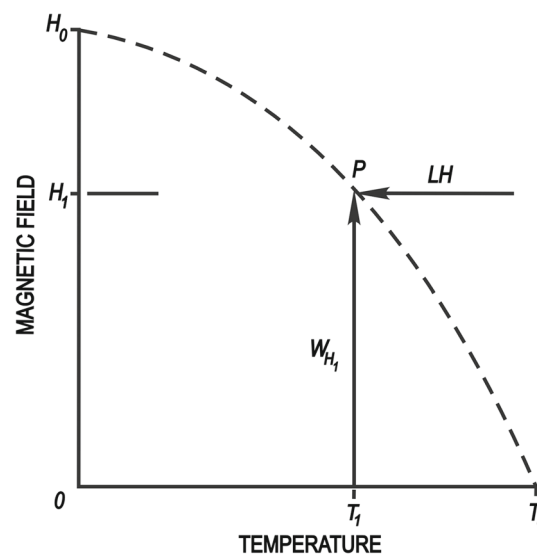


**Fig. 1**  $H$ - $T$  space diagram for an isothermal phase transition of Sn

$$W_{H_1} = \int_0^{H_1} M dH, \quad (3)$$

where  $M$  is the magnetization of the superconductor and  $H_1$  is the critical magnetic field at  $T_1$ . Phase nucleation commences at Point  $P$ ,  $H$ - $T$  space coordinate  $(H_1, T_1)$ , accompanied by a latent heat,  $LH$ , per unit volume:

$$LH = T_1 (S_n - S_s), \quad (4)$$

where  $S_n$  is the entropy of the normal phase and  $S_s$  is the entropy of the superconductive phase.

The isothermal phase transition occurs abruptly at Point  $P$ , whether the Type I superconductor is macroscopic or mesoscopic in size.

By way of example, given the superconductor is tin and  $T_1 = 0.6T_c$ , then  $H_1 = 0.64H_0$  and  $LH = 0.9216 H_0^2/8\pi$  ergs/cc.

### 2.2 Macroscopic adiabatic phase transition

In contradistinction to the isothermal phase transition, the macroscopic adiabatic phase transition from the superconductive phase to the normal phase proceeds through an intermediate state of inversely resizing volumes of superconductive and normal phase domains [10]. The relative change in superconductive phase and normal phase domain volumes proceeds isentropically according to the relation:

$$LH_{\Delta V} = \int_{T_a}^{T_b} (C_n dT) (V_n + \Delta V) + \int_{T_a}^{T_b} (C_s dT) (V_s - \Delta V), \quad (5)$$

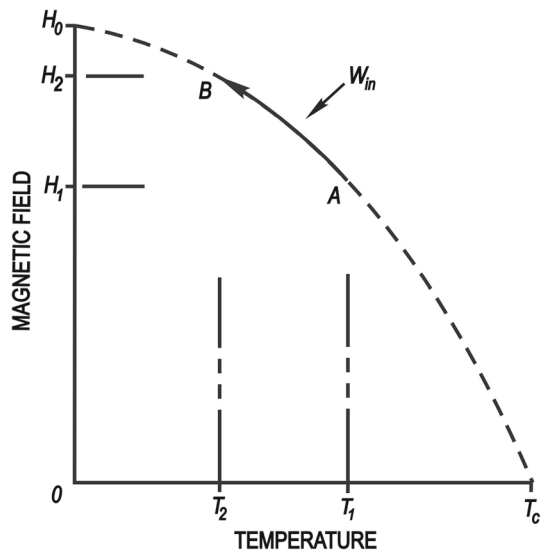


**Fig. 2**  $H$ - $T$  space diagram for a macroscopic adiabatic phase transition of Sn

where  $LH_{\Delta V}$  is the latent heat,  $C_n$  and  $C_s$  are, respectively, the specific heats of the normal and superconductive phases,  $V_n$  and  $V_s$  are, respectively, the domain volumes of the normal and superconductive phases,  $\Delta V$  is an incremental change in phase domain volume, and  $T_a$  and  $T_b$  are, respectively, beginning and ending temperatures for each  $\Delta V$ .

When the magnetic field of the sample is raised infinitesimally higher from  $H_c(T_i)$  to  $H_c + \Delta H(T_i)$ , an infinitesimal volume,  $\Delta V$  of the sample changes phase from superconductive to normal, the sample absorbing an infinitesimal latent heat,  $LH_{\Delta V}$ , which accompanies the phase transition. This results in the sample cooling as per the specific heats of the normal and superconductive domains of the volume. Now at this cooler temperature,  $T_{i-\Delta T}$ ,  $H_c + \Delta H(T_i)$  equals a new critical magnetic field of the sample,  $H_c(T_{i-\Delta T})$ .

The  $H$ - $T$  space diagram for an exemplar macroscopic adiabatic phase transition of tin is shown at Fig. 2. The magnetodynamic work performed by the source of magnetic field from zero field to  $H_1$  is given by Eq. (3).

The phase transition begins in the superconductive phase at Point A,  $H$ - $T$  space coordinate  $(H_1, T_1)$  and, passing through the intermediate state, ends in the normal phase at Point B,  $H$ - $T$  space coordinate  $(H_2, T_2)$ . Magnetodynamic work,  $W_{in}$ , is performed by the source of applied magnetic field owing to the diamagnetic screening energy associated with the superconductive domains of the intermediate state:

$$W_{in} = \int_{H_1}^{H_2} M_i dH, \tag{6}$$

where  $M_i$  is the magnetization of the superconductor in the intermediate state.

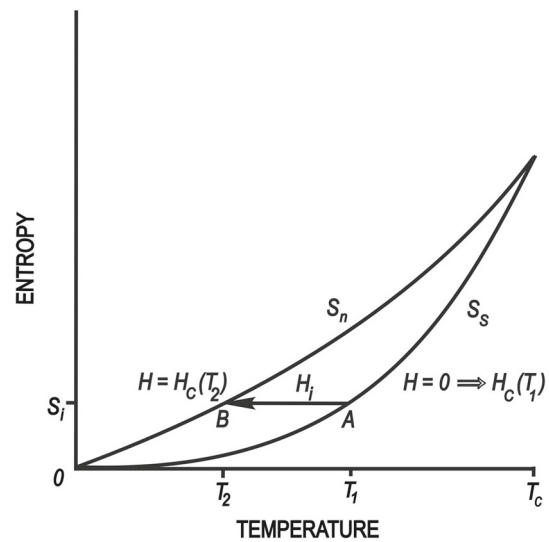


**Fig. 3**  $T$ - $S$  diagram for Sn showing a macroscopic adiabatic phase transition corresponding to Fig. 2

The phase transition from Points A to B proceeds isentropically. This follows from the fact that the phase transition is both adiabatic and, in view there is no magnetic hysteresis if performed very slowly, reversible [11].

By way of example, given the superconductor is tin and  $T_1 = 0.6T_c$ , then  $H_1 = 0.64H_0$ ,  $T_2 = 0.34T_c$ ,  $H_2 = 0.884H_0$  and  $W_{in} = 0.186H_0^2/8\pi$  ergs/cc.

A  $T$ - $S$  diagram corresponding to Fig. 2 is shown at Fig. 3, where the  $T$  axis is common.

Between Points A and B, the entropy,  $S_i$ , is constant; that is,  $S(T_i) = S(T_1) = S(T_2)$ , where  $T_i$  represents an instantaneous temperature of the intermediate state between  $T_1$  and  $T_2$ , and the instantaneous value for the magnetic field,  $H_i$ , is given by  $H_i = H_c(T_i)$ . Comparison between Figs. 2 and 3 provides a three dimensional  $H$ - $T$ - $S$  picture of the macroscopic adiabatic phase transition, where the respective  $H$  and  $S$  axes are examined utilizing the mutually corresponding  $T$  axis.

By way of example, given the superconductor is tin and  $T_1 = 0.6T_c$ , then  $H_c(T_1) = 0.64H_0$ ,  $T_2 = 0.34T_c$ ,  $H_c(T_2) = 0.884H_0$  and  $S_i = 0.401H_0^2/8\pi$  ergs/cc.

### 2.3 Mesoscopic adiabatic phase transition

In contrariety to the macroscopic adiabatic phase transition, the mesoscopic adiabatic phase transition occurs in absence of the intermediate state, owing to the specimen size being commensurate with the range of coherence,  $\xi$ , the smallest superconductive phase domain dimension [5].

Due to the absence of the intermediate state, Bardeen hysteresis will exhibit. The Bardeen hysteresis field,  $H_a$ , represents a mesoscopic adiabatic phase transition hys-

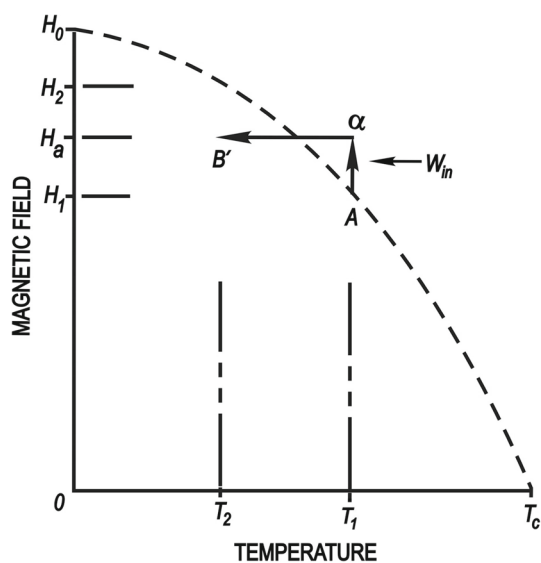


**Fig. 4**  $H$ - $T$  space diagram for a mesoscopic adiabatic phase transition of Sn

teresis field, defined by:

$$\begin{aligned} F_n(T_2) - F_s(T_1) &= \int_0^{H_1} M dH + \int_{H_1}^{H_a} M dH \\ &= H_a^2/8\pi. \end{aligned} \quad (7)$$

Figure 4 shows the  $H$ - $T$  space diagram for a mesoscopic adiabatic phase transition of tin, where, as per Fig. 2, the phase transition begins in the superconductive phase at Point A,  $H$ - $T$  space coordinate  $(H_1, T_1)$ , and the magnetodynamic work performed by the source of magnetic field from zero to  $H_1$  is given by Eq. (3).

The superconductive phase continues from Point A to Point  $\alpha$ ,  $H$ - $T$  space coordinate  $(H_a, T_1)$ . Magnetic work,  $W_{in}$ , is performed by the source of magnetic field between  $H_1$  and  $H_a$  owing to diamagnetic screening energy:

$$W_{in} = \int_{H_1}^{H_a} M dH. \quad (8)$$

Phase nucleation commences at Point  $\alpha$ , whereupon the phase transition proceeds isentropically to Point  $B'$ ,  $H$ - $T$  space coordinate  $(H_a, T_2)$ , at the respective rates of the electrodynamic and thermal relaxation times from  $T_1$  to  $T_2$ , where the term “relaxation times” relates to the specimen dimension divided by, respectively, the electrodynamic and thermal speeds of propagation. For example, aluminum has an upper limit of phonon propagation of about  $6.5 \times 10^3$  m/s [12] and a lower limit of electromagnetic wave propagation of about  $1.5 \times 10^6$  m/s [13]. The applied magnetic field remains constant at  $H_a$  from Point  $\alpha$  to Point  $B'$ .

Since  $H_a > H_c$ , the diamagnetic screening energy of the applied magnetic field above  $H_c$  will cause heating at phase nucleation, resulting in a reduction of the

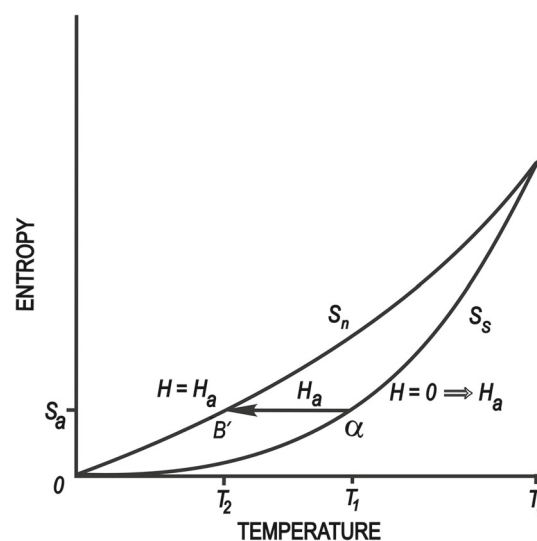


**Fig. 5**  $T$ - $S$  diagram for Sn showing a mesoscopic adiabatic phase transition corresponding to Fig. 4

latent heat of cooling,  $LH_{T_1}$ :

$$LH_{T_1} - \int_{H_1}^{H_a} M dH = \int_{T_1}^{T_2} C_n dT. \quad (9)$$

By way of example, given the superconductor is tin and  $T_1 = 0.6T_c$ , then  $H_1 = 0.64H_0$ ,  $T_2 = 0.34T_c$ ,  $H_2 = 0.884H_0$ ,  $H_a = 0.77H_0$ ,  $\pi LH_{T_1} = 0.9216H_0^2/8$  ergs/cc, and  $W_{in} = 0.186H_0^2/8\pi$  ergs/cc.

At Point  $\alpha$ , the superconductor is in the superconductive phase even though  $H_a > H_1$ . While Point  $\alpha$  appears to be the result of commonly observed (G-L/Pippard) superheating effects, a different causation of the magnetic hysteresis is involved, demonstrated by the fact that the superconductive phase at  $T_1$  persists stably and reproducibly whether the applied magnetic field is raised or lowered between  $H_1$  and  $H_a$ .

At Point  $B'$ , the superconductor is in the normal phase even though  $H_a < H_2$ . While Point  $B'$  appears to be the result of commonly observed (G-L/Pippard) supercooling effects, here also, a different causation of the magnetic hysteresis is involved, demonstrated by the fact that the normal phase at  $T_2$  persists stably and reproducibly whether the applied magnetic field is raised or lowered between  $H_2$  and  $H_a$ .

A  $T$ - $S$  diagram corresponding to Fig. 4 is shown at Fig. 5, where the  $T$  axis is common.

Between Points  $\alpha$  and  $B'$ , the entropy,  $S_a$ , is constant; that is,  $S_a(T_i) = S(T_1) = S(T_2)$ , where  $H_a$  is the Bardeen hysteresis field. Comparison between Figs. 4 and 5 provides a three dimensional  $H$ - $T$ - $S$  picture of the mesoscopic adiabatic phase transition, where the respective  $H$  and  $S$  axes are examined utilizing the mutually corresponding  $T$  axis.

By way of example, given the superconductor is tin and  $T_1 = 0.6T_c$ , then  $H_a = 0.77H_0$ ,  $T_2 = 0.34T_c$ , and  $S_a = 0.401H_0^2/8\pi$  ergs/cc.

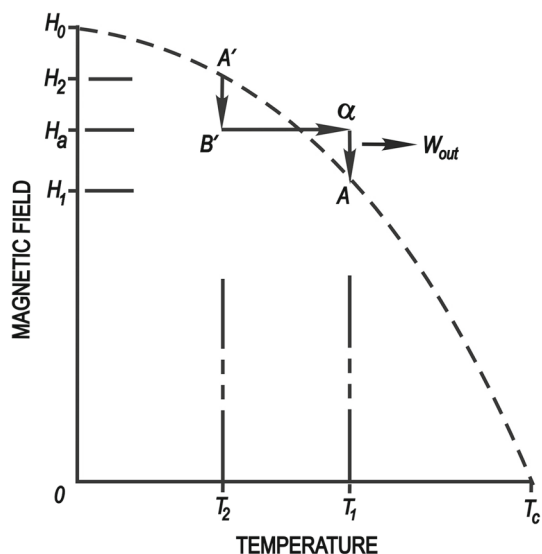


**Fig. 6**  $H$ - $T$  space diagram for a mesoscopic adiabatic phase transition of Sn in reverse of Fig. 4

An interesting aside is the reverse phase transition from the normal phase to superconductive phase, shown at Fig. 6.

Beginning in the normal phase at Point  $A'$ , the normal phase continues to Point  $B'$ . Phase nucleation commences at Point  $B'$ , whereupon the phase transition proceeds isentropically at the respective rates of the electrodynamic and thermal relaxation times, where the electrodynamic relaxation time defines the magnetodynamics of Meissner effect flux expulsion from  $T_2$  to  $T_1$ . The applied magnetic field remains constant at  $H_a$  from Point  $B'$  to Point  $\alpha$ , whereat the phase transition concludes in the superconductive phase.

With regard to attainment of Point  $A$ , the superconductive phase continues from Point  $\alpha$  to Point  $A$ . Magnetic work,  $W_{out} = -W_{in}$ , is delivered to the source of magnetic field between  $H_a$  and  $H_1$ .

Returning from the aside, Fig. 7 superposes Figs. 2 and 4.

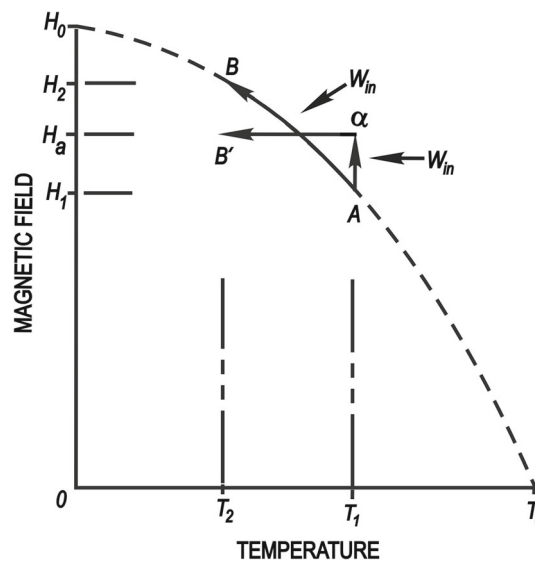


**Fig. 7** Superposition of Figs. 2 and 4

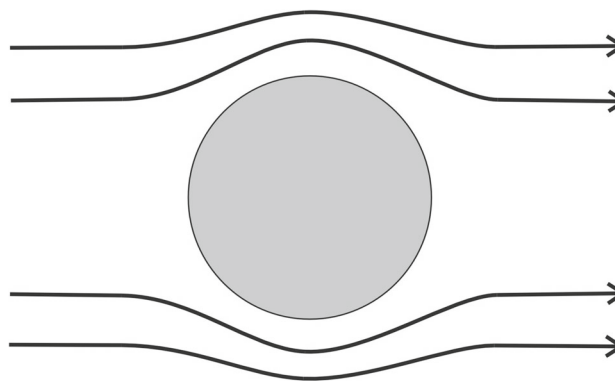


**Fig. 8** Cross-section of a superconducting wire in a transverse magnetic field

### 3 The Lutes-Maxwell experiment, a window into Bardeen hysteresis

In his letter to the Author, Bardeen remarked with regard to the mesoscopic adiabatic phase transition at  $H_1$ , "... there must be considerable 'superheating' to the higher field  $H_a$ ." It is clear magnetic hysteresis must enter the picture, but as pointed out above, the properties of Bardeen Hysteresis do not follow that of G-L/Pippard superheating. The answer to this conundrum lies in an experiment by Lutes and Maxwell investigating the magnetization of small diameter tin wires in a transverse magnetic field involving the wires' "demagnetizing factor" [14].

The demagnetization factor,  $N$ , occurs in the superconductive phase due to diamagnetic distortion of the applied magnetic field in correspondence with geometry of the sample. For a thin wire in a longitudinal magnetic field,  $N = 0$ , meaning all surfaces will homogeneously experience the same magnetic field as the applied field is raised. In Sect. 2, above,  $N = 0$ .

However, for a wire in a transverse magnetic field, as shown at Fig. 8,  $N = 1/2$ , meaning the poles will experience  $H_c$  when the equator experiences  $1/2 H_c$ .

The corresponding magnetization diagram of a macroscopic superconducting wire in a transverse magnetic field is shown at Fig. 9, where the intermediate state commences at an applied magnetic field,  $H_{int}$ , where for  $N = 1/2$ ,  $H_{int} = 0.5H_c$ .

The phase remains entirely superconductive until the applied magnetic field reaches  $H_{int}$ , then between  $H_{int}$  and the critical field,  $H_c$ , the intermediate state ensues. The progressively decreasing domain volume of the superconductive phase with respect to the progressively increasing domain volume of the normal phase is linear [10].

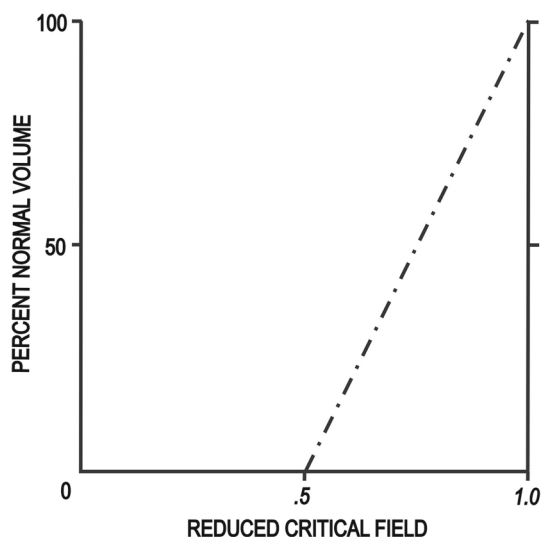


**Fig. 9** Observed magnetization diagram of a macroscopic superconducting Sn wire in a transverse magnetic field

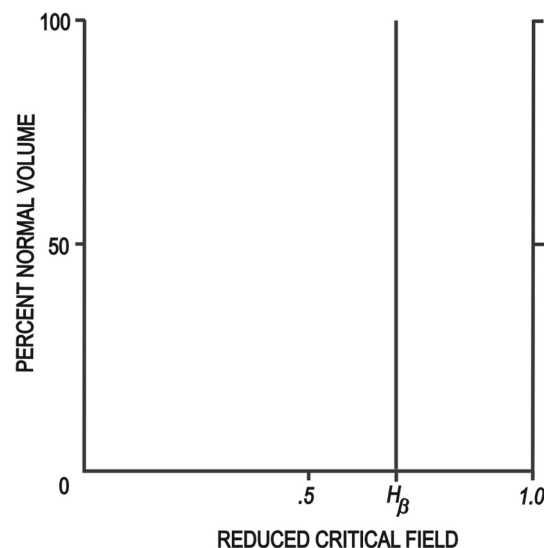


**Fig. 11** Observed magnetization diagram of a mesoscopic superconducting Sn whisker in a transverse magnetic field

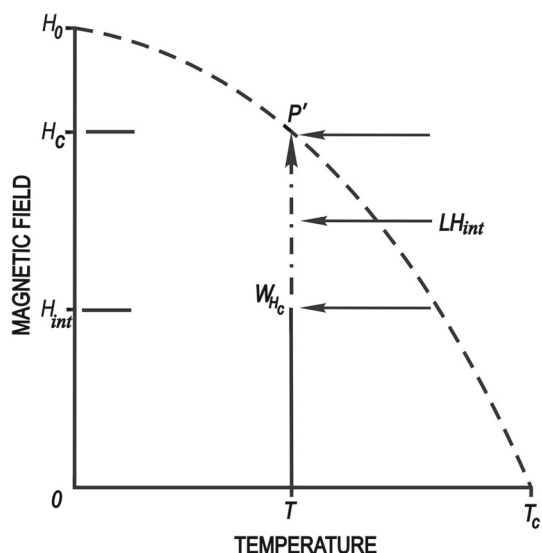


**Fig. 10**  $H$ - $T$  space diagram for an isothermal phase transition of a macroscopic Sn wire corresponding to Fig. 9

Figure 10 shows a corresponding  $H$ - $T$  space diagram for the magnetization diagram of Fig. 9.

In the superconductive phase at an arbitrary temperature,  $T$ , an applied magnetic field is raised from zero to  $H_{int}$ , whereupon the intermediate state occurs until the applied magnetic field reaches  $H_c$  at Point  $P'$ ,  $H$ - $T$  space coordinate  $(H_c, T)$ , whereat the normal phase is volumetrically complete.

In that the phase transition is isothermal, the latent heat,  $LH_{int}$ , during passage through the intermediate state is supplied by a heat reservoir between  $H_{int}$  and  $H_c$ , where now Eq. (4) applies to each incremental volume change in the normal and superconductive phase domains.

Magnetic work,  $W_{H_c}$ , is performed by the source of magnetic field owing to diamagnetic screening energy:

$$W_{H_c} = \int_0^{H_{int}} M dH + \int_{H_{int}}^{H_c} M_i dH = H_c^2/8\pi. \quad (10)$$

After first referring to prior magnetization studies for macroscopic tin wires having diameters much larger than  $\xi$  which confirm the validity of Fig. 9, Lutes and Maxwell report that for a mesoscopic tin whisker having a diameter of  $1.2 \times 10^{-4}$  cm (commensurate with  $\xi$ ), a strikingly different magnetization diagram was observed, shown at Fig. 11.

In the Lutes-Maxwell experiment, the applied magnetic field was increased from zero to  $H_\beta$ . The phase remained wholly superconductive with no appearance of the intermediate state below  $H_\beta$ . Then at  $H_\beta$ , an abrupt isothermal phase transition from the superconductive phase to the normal phase was observed, where  $H_\beta$  equalled  $0.67H_c$  and where the ambient temperature,  $T_\beta$ , equalled 1.69 K.

The  $H$ - $T$  space diagram corresponding to the result of the Lutes-Maxwell experiment is shown at Fig. 12.

In the superconductive phase at temperature  $T_\beta$ , an applied magnetic field is raised from zero to  $H_\beta$ , whereupon the phase abruptly transitions from superconductive to normal at Point  $\beta$ ,  $H$ - $T$  space coordinate  $(H_\beta, T_\beta)$ , where in Fig. 12,  $H_c$  is defined as  $H'_2$  and  $W_{H_c}$  is defined as  $W_\beta$ .

The phase transition being isothermal, the latent heat,  $LH_\beta$ , is supplied by a heat reservoir per Eq. (4).

Magnetic work,  $W_\beta$ , is performed by the source of magnetic field owing to diamagnetic screening energy:

$$W_\beta = \int_0^{H_\beta} M dH = H_\beta^2/8\pi, \quad (11)$$

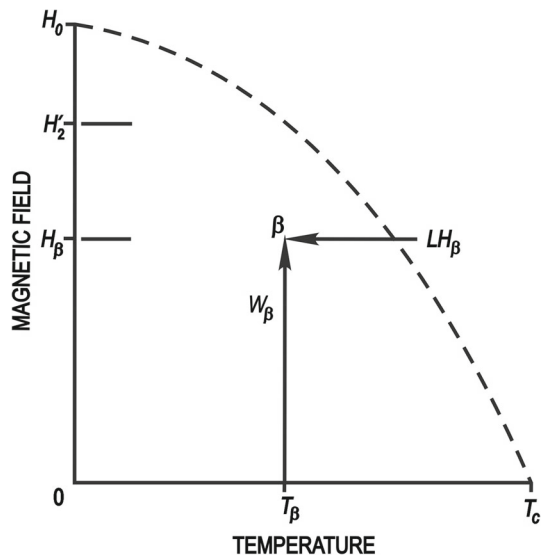


**Fig. 12**  $H$ - $T$  space diagram for an isothermal phase transition of a Sn whisker corresponding to Fig. 11

where  $H_\beta$  represents a mesoscopic isothermal phase transition hysteresis field.

Per the observations of the Lutes-Maxwell experiment, given the superconductor investigated is tin,  $T_\beta = 1.69\text{K} = 0.45T_c$ ,  $H'_2 = H_c = 0.798H_0$ , and  $H_\beta = 0.67H_c$ , then  $LH_\beta = 0.646H_0^2/8\pi$  ergs/cc.

### 3.1 Figures 4 and 12 analogues

Common to Points  $B'$  and  $\beta$ , the phase transition from the superconductive phase to the normal phase is volumetrically complete, each superconductor being in the normal phase at a respective magnetic field,  $H_a$ ,  $H_\beta$ , below the respective critical magnetic field,  $H_2$ ,  $H'_2$ , of its corresponding temperature,  $T_2$ ,  $T_\beta$ .

In that both Figs. 4 and 12 involve a mesoscopic Type I superconductor and an intermediate state that would be present but for Bardeen hysteresis,  $H_a$  and  $H_\beta$  represent Bardeen hysteresis fields for the respective mesoscopic adiabatic and mesoscopic isothermal phase transition processes; that is, in Fig. 4,  $H_a > H_1$  and in Fig. 12,  $H_\beta > H_{int}$ .

In both Figs. 4 and 12, the normal phase is not the product of commonly observed (G-L/Pippard) supercooling effects, in that the normal phase is in every respect stable and reproducible, not being subject to metastably slipping into the superconductive phase due to lattice imperfections or instabilities, as for example, fluctuations.

## 4 Discussion: Bardeen hysteresis explained

Type I superconductors exhibit a positive interphase boundary surface energy per unit volume,  $E_S$ , defined

by:

$$E_S = (1 - \lambda/\xi)(H_c^2/8\pi), \quad (12)$$

where  $\lambda$  is the penetration depth of the applied magnetic field into the surface of the superconductor and where  $\xi$  is typically an order of magnitude longer than  $\lambda$ . This positive surface energy arises at an interphase boundary because the free energy at the boundary,  $H_c^2/8\pi$ , positively changes over  $\lambda$  due to the external magnetic field contribution and negatively changes over  $\xi$  due to the superelectron contribution, where for Type I superconductors  $\lambda < \xi$  [15].

The diamagnetic screening energy per unit volume,  $E_M$ , of the superconductive phase in the presence of an applied magnetic field,  $H$ , is given by:

$$E_M = H^2/8\pi. \quad (13)$$

The condition for an interphase boundary to form is given by:

$$E_M \geq E_S. \quad (14)$$

Thus, so long as the positive interphase boundary surface energy,  $E_S$ , exceeds the diamagnetic screening energy,  $E_M$ , of the applied magnetic field, an interphase boundary cannot form and the superconductor cannot enter into the intermediate state.

Bardeen hysteresis occurs when the applied magnetic field diamagnetic screening energy required for creation of an interphase boundary exceeds  $H_c^2/8\pi$  due to the interplay between the applied magnetic field diamagnetic screening energy and the minimum energy necessary to create an interphase boundary in the presence of positive interphase boundary surface energy; that is, for  $E_S > E_M > H_c^2/8\pi$ .

Phase nucleation commences at  $H_a$  when the applied magnetic field diamagnetic screening energy equilibrates the free energies of the normal and superconductive phases (per Eq. 1). The adiabatic phase transition will proceed without appearance of the intermediate state so long as the applied magnetic field diamagnetic screening energy is less than the energy required to create an interphase boundary.

In the mesoscopic adiabatic phase transition at  $H_a$ , the entire volume,  $V$ , undergoes phase nucleation,  $E_S = E_M = H_a^2/8\pi > H_c^2/8\pi$ , and the temperature changes from  $T_1$  to  $T_2$  with a work input of  $W_{in}$ .

In the macroscopic adiabatic phase transition through the intermediate state, for each infinitesimal volume,  $\Delta V$ , of phase nucleation,  $E_S = E_M = (H_c + \Delta H)^2/8\pi$ , and for the volume  $V$ , the temperature changes from  $T_1$  to  $T_2$  with a work input of  $W_{in}$ .

### 4.1 Example 1: the mesoscopic adiabatic phase transition of Fig. 4

A numerical example follows which shows Bardeen hysteresis due to the interplay between the applied mag-

netic field diamagnetic screening energy and the minimum energy necessary to create an interphase boundary.

Free energies equilibration occurs at the mesoscopic adiabatic phase transition Bardeen hysteresis field,  $H_a$ , when:

$$F_n = F_s + H_a^2/8\pi = F_s + H_1^2/8\pi + \int_{H_1}^{H_a} M dH, \quad (15)$$

At phase nucleation the applied magnetic field energy per unit volume,  $E_M$ , is given by:

$$E_M = H_a^2/8\pi, \quad (16)$$

and the interphase boundary surface energy per unit volume,  $E_S$ , is given by:

$$E_S = (1 - \lambda/\xi)(H_2^2/8\pi), \quad (17)$$

where  $H_2$  is the critical field from  $T_1$  to  $T_2$  as a consequence of thermal relaxation.

By way of example, given the superconductor is tin and  $T_1 = 0.6T_c$ , then  $H_1 = 0.64H_0$ ,  $T_2 = 0.34T_c$ ,  $H_2 = 0.88H_0$ ,  $H_a = 0.77H_0$ ,  $W_{in} = 0.186H_0^2/8\pi$  ergs/cc,  $E_M = 0.59H_0^2/8\pi$  ergs/cc and  $E_S = 0.62H_0^2/8\pi$  ergs/cc, where for tin,  $\lambda/\xi = 0.2$  and where, because  $E_M < E_S$ , the phase transition will proceed isentropically at  $H_a$  without appearance of the intermediate state.

## 4.2 Example 2: The mesoscopic isothermal phase transition of Fig. 12

The Lutes–Maxwell experiment provides experimental evidence for Bardeen hysteresis arising from the interplay between the the applied magnetic field diamagnetic screening energy and the minimum energy necessary to create an interphase boundary, as follows.

Free energies equilibration was observed by Lutes and Maxwell at the mesoscopic isothermal phase transition Bardeen hysteresis field,  $H_\beta$ , when:

$$F_n = F_s + H_2'^2/8\pi = F_s + \int_0^{H_\beta} M dH. \quad (18)$$

The numerical values observed in the Lutes–Maxwell experiment on a tin whisker are:  $H_{int} = 0.5H_2'$ ,  $T_\beta = 0.45T_c$  and  $H_\beta = 0.67H_2'$ . Therefore,  $H_2' = 0.798H_0$ ,  $H_\beta = 0.535H_0$  and  $W_\beta = 0.637H_0^2/8\pi$  ergs/cc.

At phase nucleation the applied magnetic field energy per unit volume,  $E'_M$ , is given by:

$$E'_M = H_\beta^2/8\pi, \quad (19)$$

and the interphase boundary surface energy per unit volume,  $E'_S$ , is given by:

$$E'_S = (1 - \lambda/\xi)(H_2'^2/8\pi), \quad (20)$$

where, per the aforesaid numerical values,  $E'_M = 0.286H_0^2/8\pi$  ergs/cc and  $E'_S = 0.51H_0^2/8\pi$  ergs/cc. Accordingly, since  $E'_M < E'_S$ , the phase transition was observed to proceed abruptly at  $H_\beta$  without appearance of the intermediate state.

## 5 Conclusion

The causation of Bardeen hysteresis in the first order adiabatic phase transition of a mesoscopic Type I superconductor relates to a minimum required applied magnetic field diamagnetic screening energy to create an interphase boundary.

Bardeen hysteresis occurs when the applied magnetic field diamagnetic screening energy required for creation of an interphase boundary exceeds  $H_c^2/8\pi$  due to the interplay between the applied magnetic field diamagnetic screening energy and the minimum energy necessary to create an interphase boundary in the presence of positive interphase boundary surface energy.

Phase nucleation commences when the applied magnetic field diamagnetic screening energy equilibrates the free energies of the normal and superconductive phases. The adiabatic phase transition will proceed without appearance of the intermediate state so long as the applied magnetic field diamagnetic screening energy is less than the energy required to create an interphase boundary.

The Lutes–Maxwell experiment, which investigated the isothermal phase transition of a mesoscopic tin whisker in a transverse magnetic field ( $N=1/2$ ), showed an abrupt phase transition absent appearance of the intermediate state. The magnetic field at which the transition occurred provides experimental evidence for Bardeen hysteresis arising from the interplay between the applied magnetic field diamagnetic screening energy and the minimum energy necessary to create an interphase boundary in the presence of positive interphase boundary surface energy.

**Open Access** This article is licensed under a Creative Commons Attribution 4.0 International License, which permits use, sharing, adaptation, distribution and reproduction in any medium or format, as long as you give appropriate credit to the original author(s) and the source, provide a link to the Creative Commons licence, and indicate if changes were made. The images or other third party material in this article are included in the article's Creative Commons licence, unless indicated otherwise in a credit line to the material. If material is not included in the article's Creative Commons licence and your intended use is not permitted by statutory regulation or exceeds the permitted use, you will need to obtain permission directly from the copyright holder. To view a copy of this licence, visit <http://creativecommons.org/licenses/by/4.0/>.



## References

1. J. Bardeen, private letter communication to P.D. Keefe, Loomis Laboratory of Physics, Univ. of IL Archives, Record series: box 28 of the Bardeen papers
2. P.D. Keefe, Quantum mechanics and the second law of thermodynamics: an insight gleaned from magnetic hysteresis in the first order phase transition of an isolated mesoscopic-size Type I superconductor. *Phys. Scripta* **T151**, 014029 (2012)
3. J. Feder, D.S. McLachlan, Superheating and supercooling in single spheres of tin, indium, and gold-plated indium. *Phys. Rev.* **177**(2), 763 (1969)
4. H.L. Caswell, Magnetic hysteresis in superconducting thin films. *J. Appl. Phys.* **36**(1), 80 (1965)
5. A.B. Pippard, XXI. Magnetic hysteresis in superconducting colloids. *Philos. Mag.* **43**(338), 273 (1952)
6. T. Tsuboi, T. Suzuki, Specific heat of superconducting fine particles of tin; I. fluctuations in zero magnetic field. *J. Phys. Soc. Jpn.* **42**(2), 437 (1977)
7. D.H. Douglass Jr., Magnetic field dependence of the superconducting energy gap. *Phys. Rev. Lett.* **6**(7), 346 (1961)
8. C.A. Bryant, P.H. Keesom, Low-temperature specific heat of indium and tin. *Phys. Rev.* **123**(2), 491 (1961)
9. F. London, *Superfluids*, vol. 1, 2nd edn. (Dover Publications, New York, 1961), pp. 16–26
10. R.L. Dolecek, Adiabatic magnetization of a superconducting sphere. *Phys. Rev.* **96**(1), 25 (1954)
11. M. Yaqub, Cooling by adiabatic magnetization of superconductors. *Cryogenics* **1**(2), 101 (1960)
12. *CRC Handbook of Chemistry and Physics*, 51st edn, ed. by R.C. Weast (Chemical Rubber Co., Cleveland, 1970–71), p. E411
13. J. Bartl, M. Baranek, Emissivity of aluminum and its importance for radiometric measurement. *Meas. Sci. Rev.* **4**, 31 (2004)
14. O.S. Lutes, E. Maxwell, Superconducting transitions in tin whiskers. *Phys. Rev.* **97**, 1718 (1955)
15. A.C. Rose-Innes, E.H. Rhoderick, *Introduction to Superconductivity*, 2nd edn. (Pergamon Press, Oxford, 1978), pp. 77–81